Arab J. Nucl. Sci. Appl., Vol. 57, 3, 35-43 (2024)

ISSN 1110-0451

Arab Journal of Nuclear Sciences and Applications

Web site: ajnsa.journals.ekb.eg

(E S N S A)

Analysis of Small Modular SMART Reactor Core Fuel Burn up using MCNPX code

Moustafa Aziz

Department of Nuclear Safety Engineering, Nuclear and Radiological Safety Research Center, Egyptian Atomic Energy Authority, Cairo, Egypt

ARTICLE INFO

Article history:

Received: 17th May 2024

Accepted: 23rd June 2024

Available online: 3rd July 2024

Keywords:

SMART Reactor;
MCNPX Code;
Neutronic Analysis;
Fuel Burnup.

ABSTRACT

SMART Nuclear reactor, which is conceptually developed by KAERI (Korea Atomic Energy Research Institute), is a Small modular reactor of 330 Mwth. MCNPX computer code Package which is based on Monte Carlo method is used to model the reactor core and evaluate neutronic characteristics of the core. Reactor multiplication factor is evaluated with time. Fuel burnup and depletion of fissile ^{235}U and breeding of plutonium are calculated with fuel burnup along the life cycle of the reactor core. Radial and axial Power and flux mapping distributions are calculated along all fuel assemblies of the core. Delayed neutron fraction, prompt neutron life time as well as fuel, moderator and void temperature coefficient of reactivity are evaluated and analysed. The results indicated that average core burnup extends to 27 GWd/T after 3 operation years which corresponds to ^{235}U burnup ratio of 71 %. Power distribution is compared to previously published results and satisfactory agreements were found

I- INTRODUCTION

SMART reactor which is designed by KAERI (Korea Atomic Energy Research Institute), is a small-sized integral and modular Pressurized water reactor that produces 90 MWe of electric power under full operating conditions. Major parts including primary circuit pumps, steam generators and a pressurizer are installed within the pressure vessel, in which the distribution of components differs from the traditional pressurized water reactor [1].

The SMART design is an advanced and multipurpose reactor. It can be used for electricity production and sea water desalination especially in remote and isolated electric grid. The SMART has a daily load following capacity that can be finely controlled by combining with the amount of seawater desalination. Passive safety systems control safety and accident mitigation and progression, so safety and security of the reactor could be achieved without off site power [2,3,4]. Figure 1 illustrates the main component of the reactor. The core contains 4 (MCP) main coolant pump which are installed vertically at the top of the reactor, PZR a self pressurizer, CEDM Control rod drive mechanism, SG Steam generator located at the circumferential periphery between the core support barrel and the RPV above the core. The design eliminates the primary coolant pipes and minimize the possibility of both (LBLOCA) large loss of coolant accident and (SBLOCA) small loss of coolant accident [5,6,7,8,9]

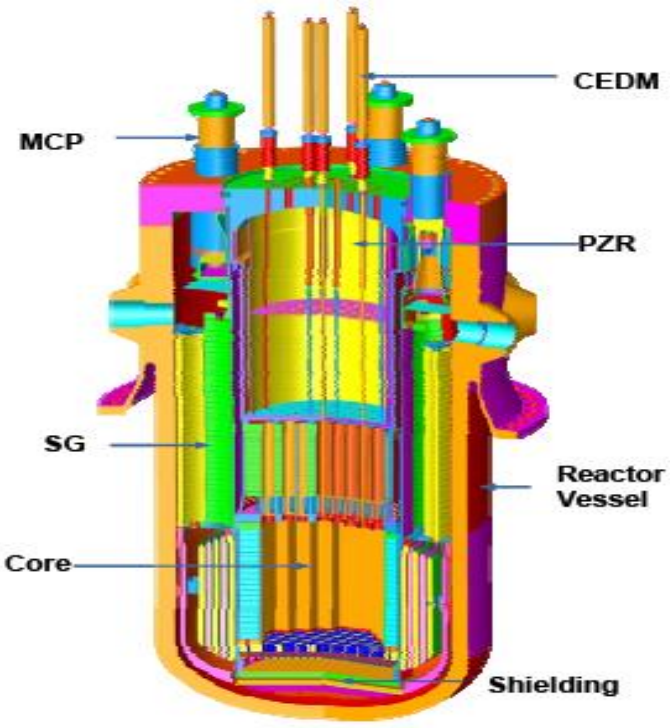

Fig. (1): SMART Core and pressure Vessel

Corresponding author: moustafaaai@yahoo.com
DOI: 10.21608/AJNSA.2024.290367.1819

II- CORE DATA ANALYSES

The SMART core is composed of 57 fuel assemblies and each assembly 17x17 fuel rods. The cycle length approximately 990 operation days with average cycle burnup of 26,500 MWd/T. The core is free from soluble boron, and this simplifies the volume and chemical control system. The reactor uses Uranium dioxide (UO_2) with enrichment 4.95 % for all assemblies and burnable poisons are used to suppress the initial reactivity of the fuel. Due to the use of various burnable absorbers, the fuel assemblies are classified into 4 different sub-batches according to the type and Number of burnable poisons rods in each assembly. Table 1 illustrates four fuel batches (A , B,C and D) with the number of assemblies in the core and number of fuel and burnable poisons rods per assembly. Figure 2 illustrates the distribution of fuel assembly types in the reactor core [2].

Table (1): Fuel assembly distributions in the core [8]

Assembly Type	Number of assembly	No. of fuel rod	No. of Al_2O_3- B_4C	No. of Gd_2O_3-UO_2
A	20	240	24	-
B	16	244	20	-
C	1	236	24	4
D	20	228	24	12

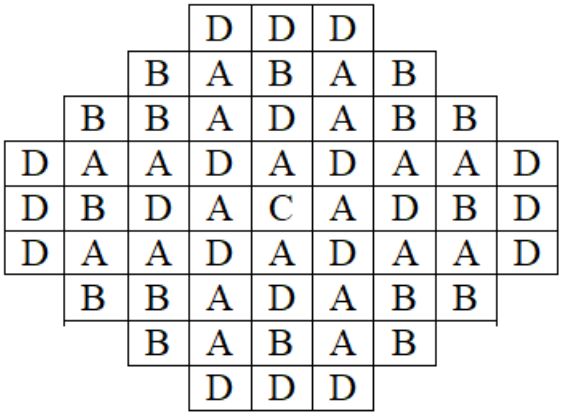

Fig. (2): SMART core loading pattern

II.1 Control Rods and Burnable Absorbers

The core contains 41 control assembly divided into two groups of control rods : Regulating rods composed of Ag-In-Cd and are divided into 3 banks R1, R2 , and R3. Shutdown rods composed of B_4C and are divided into 5 banks S1, S2, S3, S4, and S5.

Two types of burnable absorbers; $A1_2O_3$-B4C and Gd_2O_3 are used to adjust the criticality of the reactor. $A1_2O_3$-B4C burnable absorbers with B-10 concentrated to 30 w/o are used in every fuel assembly (Table 1). Additionally, gadolinia fuel rods are used in some fuel assemblies to enhance the safety shutdown margin at BOC. The gadolinia fuel rod is composed of Gd_2O_3 of 12 w/o admixed in UO_2 of 1.8 w/o U-235 [1,2]. Table 2 contains core and fuel data [2]. Table 3 contains Burnable poisons data.

Table (2): Core and Fuel data [2]

Parameter	value
Thermal power Mwth	330
Inlet/outlet coolant temperature	270/310 ^oC
Primary circuit pressure	15 Mpa
Peaking factor	3.6
Specific power	26.535 Mw/T
No. of fuel assemblies	57
No. of Control assemblies	41
Fuel rod arrays	17 x17
rod pitch	1.26 cm
Pellet radius	0.401 cm
Pellet density	10.4 g/cm^3
Clad materials	Zircaloy -4
Clad inner radius	0.411
Clad outer radius	0.475 cm
Active core height	200 cm
Assembly dimensions	21.4x21.4 cm
Fuel materials	UO_2

Table (3): Burnable Poisons Data

parameter	Al_2O_3-B_4C	Gd_2O_3-UO_2
Pellet rod diameter	0.7604 cm	0.804 cm
Pellet density	3.94 g/cm^3	9.748 g/cm^3
UO_2 theoretical density	-	10.96 g/cm^3
Gd_2O_3 density	-	7.41 g/cm^3
clad	Zircaloy	Zircaloy
Clad inner radius	0.411 cm	0.411 cm
Clad outer radius	0.475 cm	0.475 cm

III- Computer Model

MCNPX Computer code [10] is used to model whole SMART core with all details of fuel, control rods and burnable poisons are incorporated in the model. Burnup cards are activated in the model to analyse the time

dependent fuel burnup. Figure 3 (a,b,c and d) represents code model to type A,B,C, and D fuel assembly Batches. Figure 4 MCNPX code model to the whole reactor core.

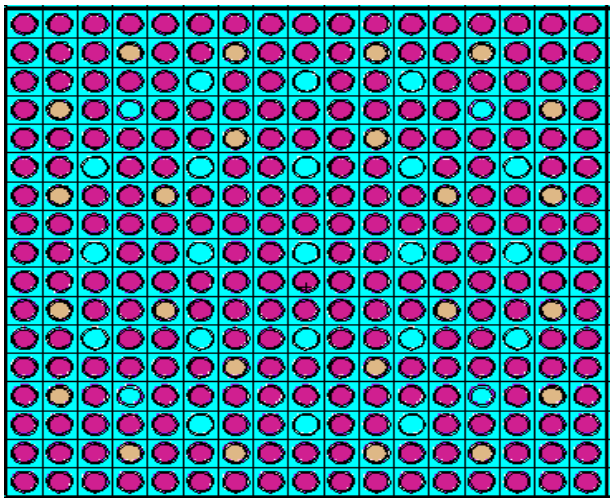

Fig. (3.a): Computer model for Type A fuel Batch

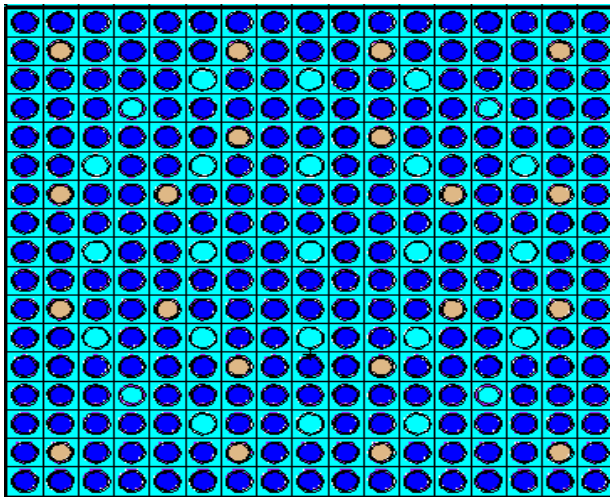

Fig. (3.b): Computer model for Type B fuel Batch

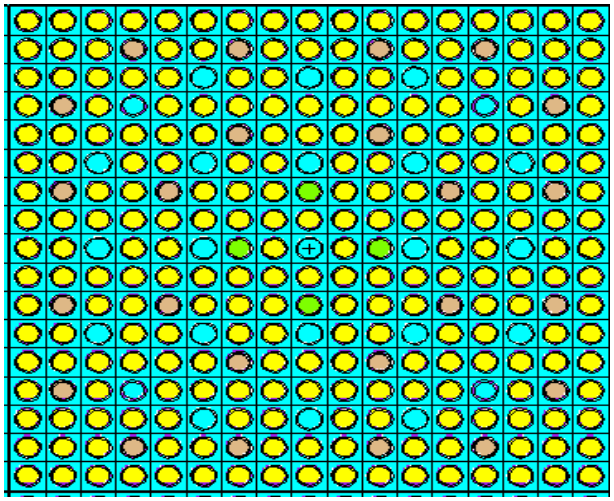

Fig. (3.c): Computer model for Type C fuel Batch

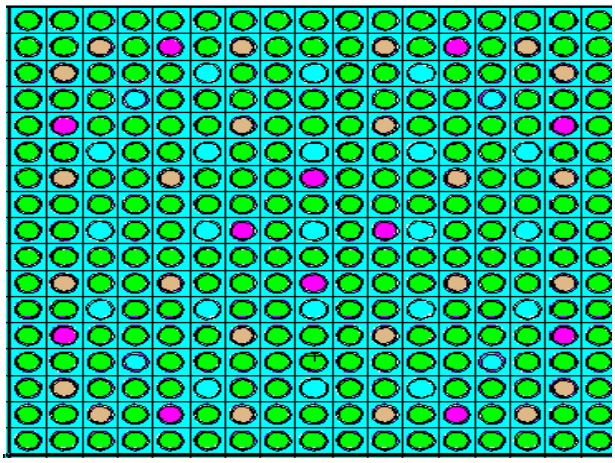

Fig. (3.d): Computer model for Type D fuel Batch

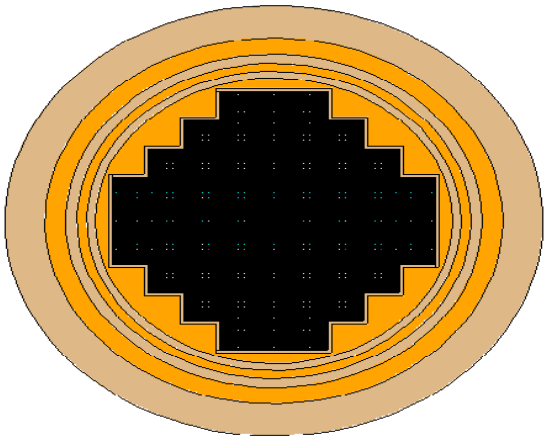

Fig. (4): MCNPX Horizontal model to the reactor Core

IV- RESULTS AND DISCUSSIONS

Figure 5 illustrates core multiplication factor K_{eff} versus operation time (day) , the initial K_{eff} =1.14988 at time t=0.0, then it decreases due to fission products and Xenon formation . after that there are two competitive process; burnable poison burnup which release positive reactivity to the core, and fuel burn up which leads to negative reactivity and reduction of multiplication factor. Core cycle length extends to 3 years.

Figure 6 Fuel Burnup (Gwd/T) Versus Operation times (days) for different Core Zones A, B, C,, D and average core burnup (Gwd/T). The results indicate that the discharge burnup for fuel batch type A, B, C, D and average core are 40.5 ,29.3 , 49.7 , 27 and 32.9 GWd/T respectively. The results show that fuel Batch C the central assembly is the higher burnup , average core burnup is higher than batches B and D.

Figure 7 illustrates ^{235}U (atom/barn. cm) versus operation time (days) for the reactor core. ^{235}U initial concentration $1.163x10^{-3}$ (atom/barn.cm) which reduces to $3.4x10^{-4}$ with ratio of 0.29 which means that 71 % of ^{235}U is consumed.

Figure 8 illustrates fissile plutonium (atom/barn. cm) versus operation time (days) for the reactor core. ^{239}Pu at the end of cycle (EOC) is $1.47x10^{-4}$ (atom/barn.cm) , ^{241}Pu (EOC)= $2.75x10^{-5}$ and total plutonium is $1.75x10^{-4}$ (atom/barn.cm) at EOC.

Figure 9 illustrates power assembly normalized to average value as calculated by present MCNPX model and the results obtained by reference [2]. Higher values for present MCNPX calculations and lower for the reference.

Figure 10 illustrates Power Mapping distribution through reactor core, the results are normalized to the average core power (which is total power divided by Number of assemblies 330/57) , Maximum power peaking factor is 1.581 which occur at central assembly type C. The power is higher at core center and reduces in the outer assemblies. The minimum assembly power is 0.271.

Figure 11 illustrates thermal flux Mapping distribution through reactor core, the results is divided by 10^{13} ,maximum thermal flux $3.079x10^{13}$ n/cm^2.s and minimum thermal flux is $0.595x10^{13}$. the thermal flux is higher at core center and lower towards core periphery.

IV-1 Kinetic and Safety Coefficients

Table 4 illustrates delayed neutron fraction (β) and prompt neutron life time. The delayed neutron fraction is 704 pcm and prompt neutron life time is 21.6 μs. The delayed neutron fraction (β) is calculated from the relation:

$$\beta = 1 - \frac{K_p}{K_{eff}}$$

Where K_p reactor multiplication factor with prompt neutrons only , K_{eff} multiplication factor with total neutrons considered (prompt and delayed). Prompt neutrons life time is built –in results from MCNPX code.

Table 5 illustrates fuel temperature coefficient of reactivity α_f (pcm/k) , moderator temperature coefficient (pcm/k) and void coefficient. Fuel temperature coefficient of reactivity indicates negative behavior and equal -2.0528 pcm/k fuel coefficient due to Doppler broadening during temperature rise. α_f calculated from the relation:

$$\alpha_f = \frac{\Delta K}{k_1\, k_2\, \Delta T}$$

ΔT the difference between temperature T_2 and T_1 , with corresponding multiplication factor K_2 and K_1 respectively. ΔK the difference between factor K_2 and K_1.

Moderator coefficient of reactivity measures the reactivity change due to temperature and coolant density change, the average value for this coefficient is negative and equal -56.04 pcm/k. Figure 12 illustrates the variation of core K_{eff} versus fuel temperature. The temperature and fluid (water) density are calculated at temperature 300 C , 310 C , 320 C , 330 C and 350 C and the corresponding water density is incorporate at the MCNPX input to calculate the corresponding K_{eff}.

Figure 12 illustrates that K_{eff} reduces with increasing temperature. Table 5 also shows void coefficient of reactivity for 100 % void. Void coefficient is calculated as the difference between multiplication factor at normal states and the second state which the core is void (void core at which water density is divided by 10 approximately equal to steam density) the results indicate that void coefficient of reactivity is very large negative because of loss of moderator. Which equal -65061pcm for 100 % $\frac{\Delta V}{V}$ $void$.

Figure 13 illustrates Axial thermal flux (n/cm^2.s) versus core height (axial distance negative values represent core bottom) Maximum flux occurs at central assembly type C with Maximum value of $4.36x10^{13}$ (n/cm^2.s) at core center while flux maximizes. Axial flux is lower at assemblies of type A, B and D and thermal flux is lower at theses assemblies because it is far from core center. Figure 14 illustrates axial power peaking factor at assemblies of batches A, B, C, and D respectively. Maximum power peaking of 2.48 which occurs at core centerline.

Figure 15 illustrates average B-10 in the core (atom/barn.cm) versus operation time (day), Burnable poison B-10 reduces with operation time, three values are interesting at time t=0.0 days (initial concentration) $=5.55x10^{-4}$ (atom/barn.cm). And at t=400 days the concentration equals $2.78x10^{-5}$ which corresponds the peak value in Figure 5, and the discharge value $1.123x10^{-12}$ (atom/barn.cm).

V- CONCLUSION

- MCNPX computer Code is used to model SMART Reactor core, time dependent module is employed and Fuel burnup is calculated and analysed. The results indicated that core cycle length is 3 years with average core burn up extends to 27 Gwd/T.
- ^{235}U burnup ratio is 71 % while total fissile Plutonium is $1.75x10^{-4}$ atom/barn.cm.
- Axial flux calculation indicates that Max power is 2.48 with flux equal $4.36x10^{13}$ n/cm^2.s

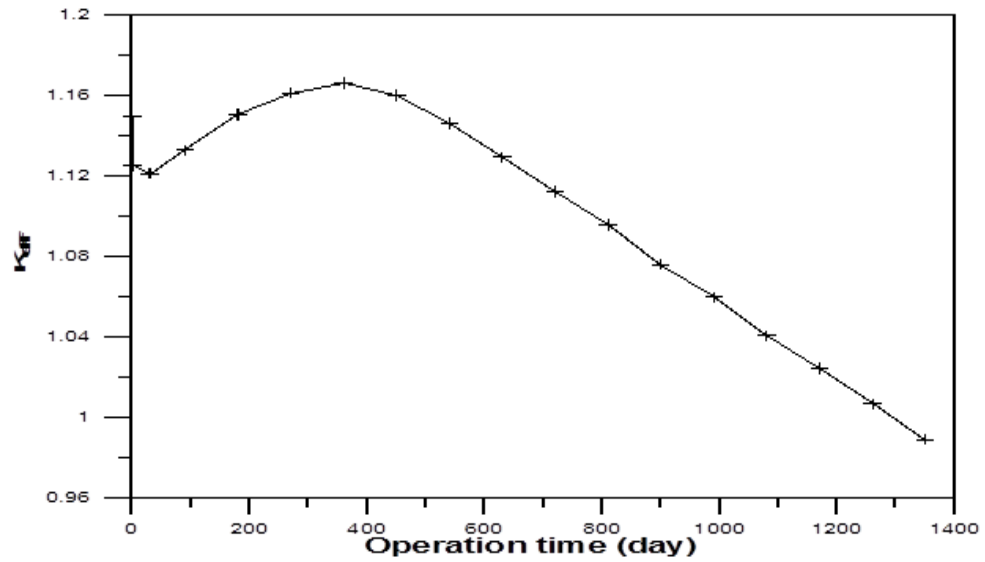

Fig. (5): K_{eff} versus operation time (day) for the reactor core

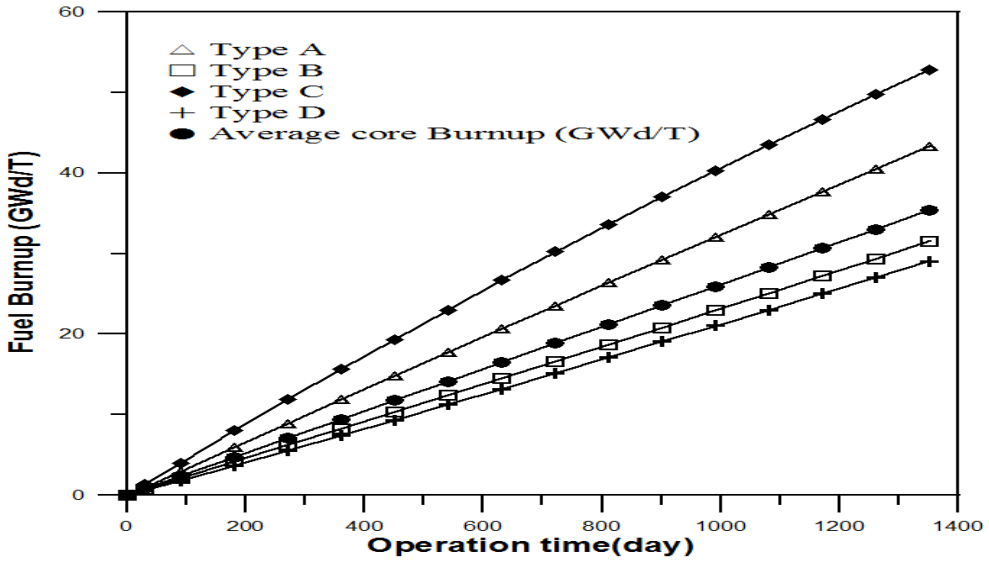

Fig. (6): Fuel Burnup (Gwd/T) Versus Operation times (days) for different Core Zones

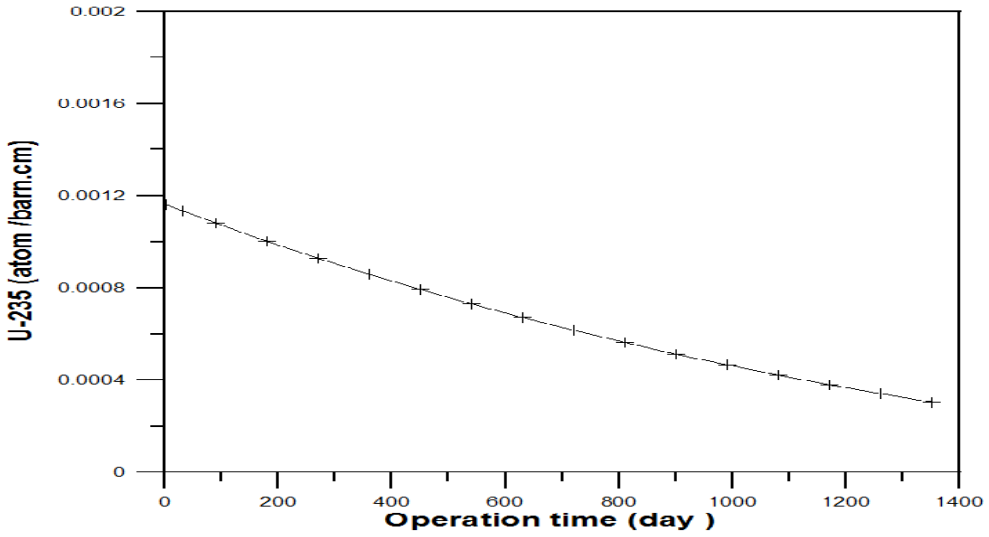

Fig. (7): ^{235}U (atom/barn. cm) versus operation time (days) for the reactor core

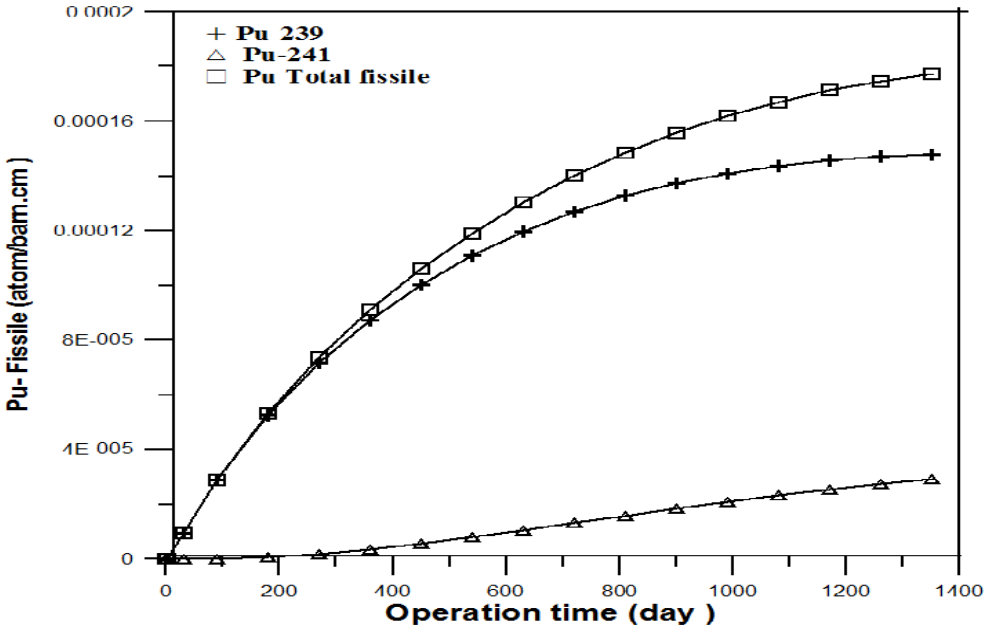

Fig. (8): Fissile plutonium (atom/barn. cm) versus operation time (days) for the reactor core

1.581 1.45	1.334 1.455	1.152 1.216	0.98 1.134	0.365 0.467
1.567 1.455	1.336 1.291	1.293 1.351	0.874 1.024	0.300 0.38
1.219 1.216	1.329 1.351	1.117 1.280	0.595 0.766	
1.012 1.134	0.916 1.024	0.627 0.766		
0.368 0.467	0.305 0.380			

Fig. (9): Comparison Between present MCNPX model (upper value) and Reference (lower value)

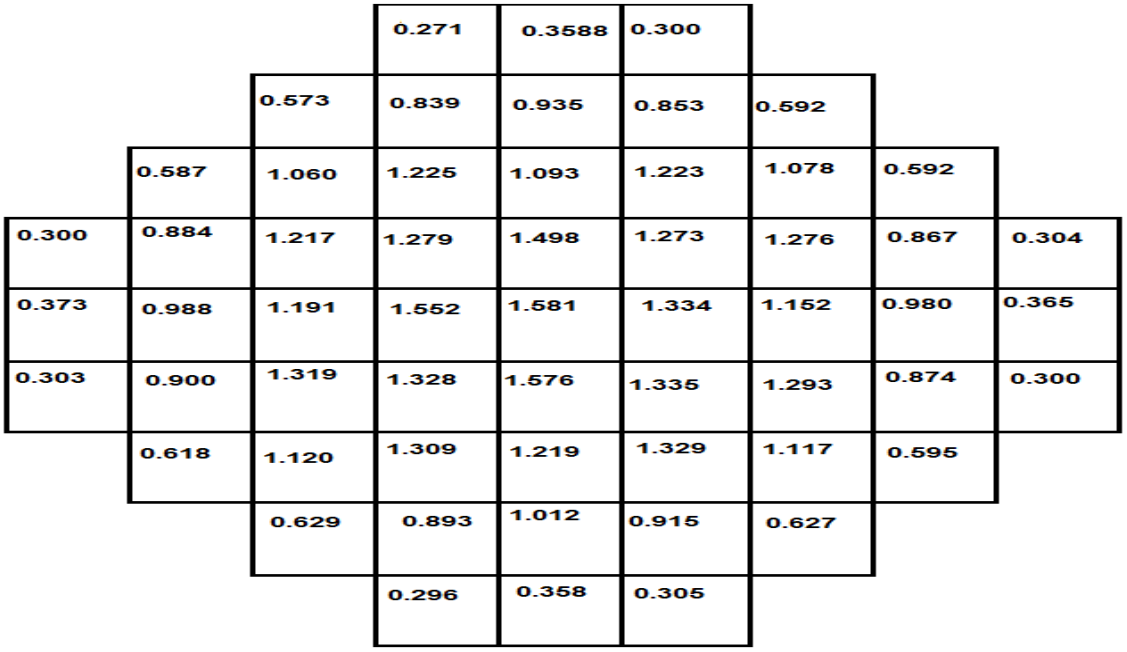

Fig. (10): Power Mapping distribution through reactor core

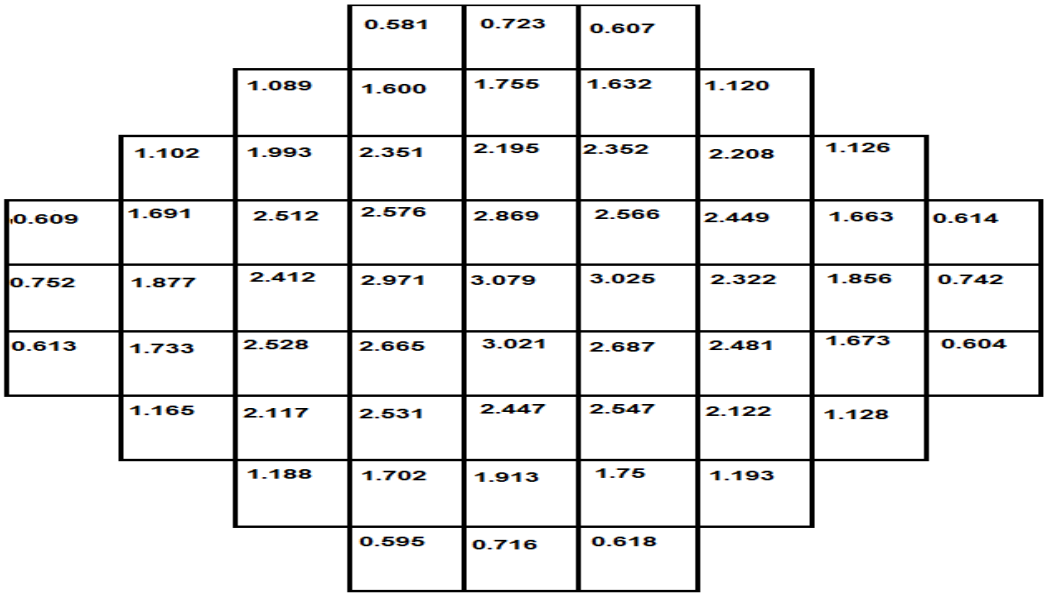

Fig. (11): Thermal flux Mapping distribution through reactor core (normalized to 10^{13})

Table (4): kinetic parameters for SMART Core

Delayed fraction (β)	Prompt life time life time (μs)
704 pcm	21.6 μs

Table (5): Safety parameters for SMART reactors

Fuel coefficient of reactivity pcm/°K	Moderator Coefficient of reactivity pcm/°K	Void Coefficient pcm
-2.0528 pcm/k	-56.04 Pcm /K	-65061 pcm for 100 % void

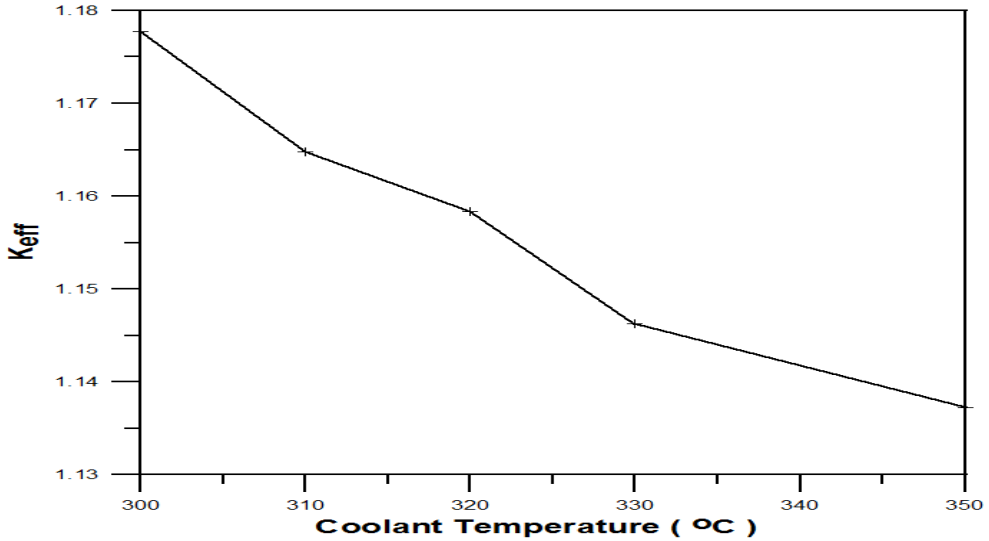

Fig. (12): Reactor K_{eff} versus coolant temperature (ºC)

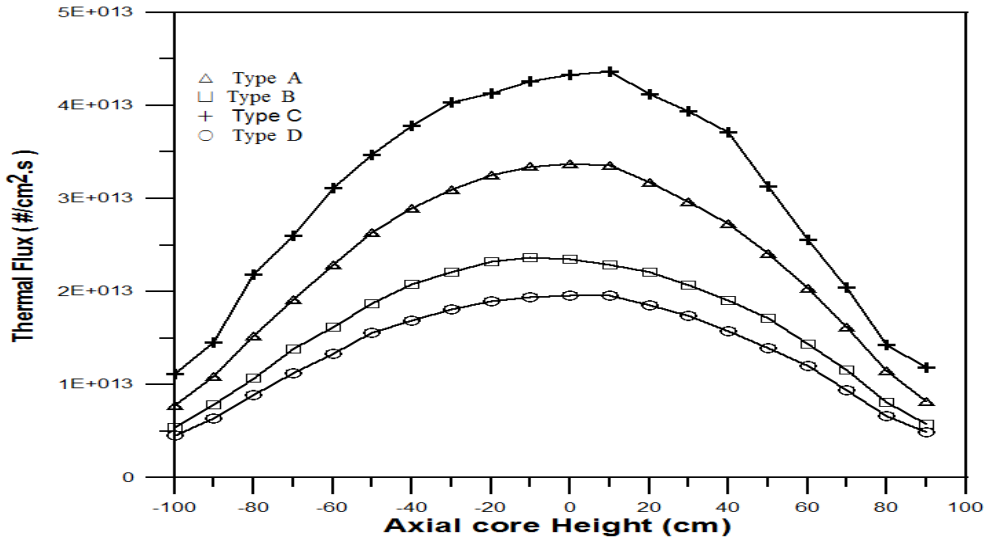

Fig. (13): Axial Flux Distributions Through Different fuel Regions for SMART Core

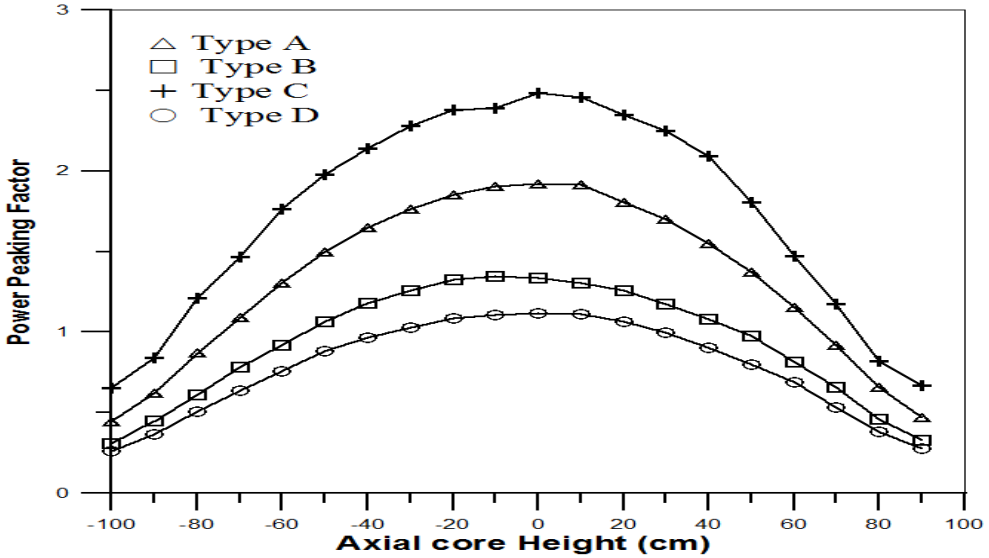

Fig. (14): Axial Power normalized Through Different fuel Regions for SMART Core

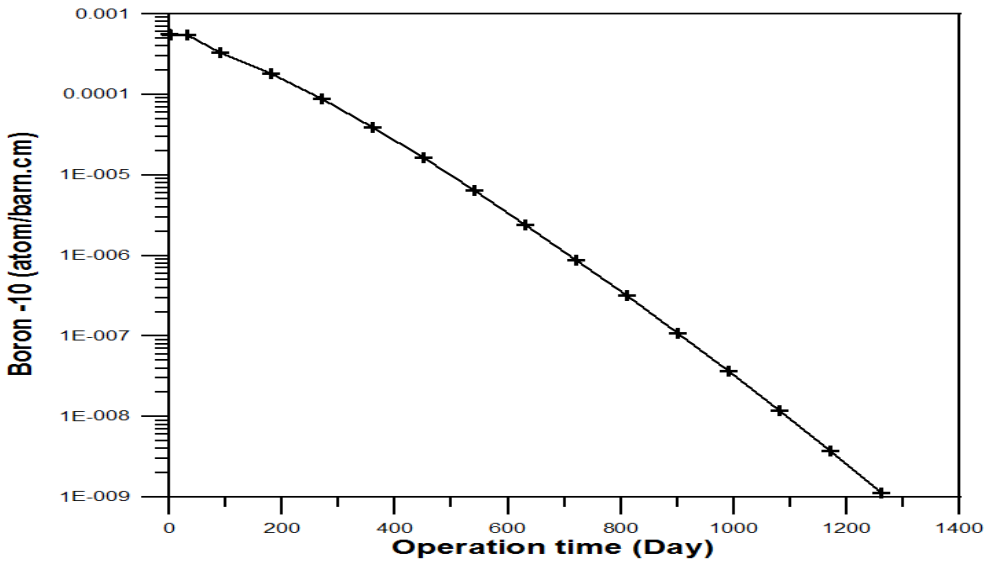

Fig. (15): B-10 (atom/barn.cm) versus operation time (day)

VI- REFERENCES

[1] Status report 77 - System-Integrated Modular Advanced Reactor (SMART)

[2] KAERI/TR-1162/98, Nuclear Characteristics Analysis Report for System-integrated Modular Advanced Reactor Korea Atomic Energy Research Institute (1998)

[3] Khurram Mehboob, Yahya A. Al-Zahrani· Abdulsalam Alhusawai1,· Majid Ali Neutronic Analysis of SMART Reactor Core for (U-Th)O2 and MOX Fuel Hybrid Configurations. Arabian Journal for Science and Engineering, January 2023, https://doi.org/10.1007/s13369-022-07541-7

[4] Jaejun Lee , Jong Hyuck Won , Nam Zin Cho , Yong Ho Ryu , and Ju Yeop Park, A Preliminary Analysis of SMART Reactor Core Using the COREDAX Code. Transactions of the Korean Nuclear Society, Autumn Meeting Jeju, Korea, October 21-22, 2010

[5] Yiming Zhong , Paul Norman and Wenbin Wu, A Feasibility Study of SMART Reactors Power performance optimizations-Part 1: Steady State and Burnup Ansalysis. Fronters in Energy Research. 1-12, 30 Augest 2022, Doi.10.3389 , fenrg 2022,976602

[6] Yiming Zhong , Paul Norman and Wenbin Wu, A Feasibility Study of SMART Reactors Power performance optimizations-Part 2: Reflector Material Selection. Fronters in Energy Research . 1-12, 30 Augest 2022, Doi 10.3389, fenrg 2022,987515

[7] Rahmi N. Ramdhani1 , Puguh A. Prastyo1 , Abdul Waris,, Widayani and Rizal Kurniadi, Neutronics Analysis of SMART Small Modular Reactor using SRAC 2006 Code. IOP Conf. Series: Journal of Physics: Conf. Series 877 (2017) 012067 doi :10.1088/1742- 6596/877/1/012067

[8] Rahmi N. Ramdhani1 , Abdul Waris, Widayani and Rizal Kurniadi. Study on SMART Reactor Design Using ThO2-UO2 Fuel. IOP Conf. Series: Journal of Physics: Conf. Series 1127 (2019) 012025 doi:10.1088/1742-6596/1127/1/012025

[9] Keung Koo Kim, Wonjae Lee, Shun Choi, Hark Rho Kim and Jaejoo Ha, SMART: The First Licensed Advanced Integral Reactor , Journal of Energy and Power Engineering 8 (2014) 94-102

[10] Hendricks J. S. et.,al. MCNPX2.6D Computer Code package. Los Alamos National Lab. (2007) LA-UR 074137.